

Regular article

Generalization of the nonlocal resonance model for low-energy electron collisions with hydrogen halides: the variable threshold exponent*

J. Horáček¹, M. Čížek¹, W. Domcke²

¹Faculty of Mathematics and Physics, Charles University, CZ-180 00 Praha 8, Czech Republic

²Institute of Theoretical Chemistry, Heinrich-Heine-University, D-40225 Düsseldorf, Germany

Received: 14 May 1998 / Accepted: 27 July 1998 / Published online: 9 October 1998

Abstract. The nonlocal resonance model developed previously for the description of low-energy electron collisions with hydrogen halides is generalized to include the dependence of the dipole-modified threshold exponent on the internuclear distance. An efficient computational scheme has been developed to deal with the resulting nonseparability of the nonlocal complex potential for the nuclear motion within the Schwinger-Lanczos approach. The results reveal that the R -dependence of the threshold exponent has a significant effect on the threshold peaks in the vibrational excitation cross sections of HCl. The shape and intensity of the calculated threshold peak in the $0 \rightarrow 1$ vibrational excitation channel, in particular, are in much better agreement with experimental data than previous results. For the electron-HBr and electron-HI collision systems the effects of the R -dependence of the threshold exponent are not significant.

Key words: Electron – molecule scattering – Threshold phenomena – Resonance – Nonlocal complex potential

1 Introduction

Pronounced and unusual threshold structures in the vibrational excitation (VE) and dissociative attachment (DA) cross sections of the hydrogen halides HF, HCl, and HBr were discovered more than 20 years ago [1–3]. The excitation functions of the low vibrational levels exhibit intense and narrow peaks at threshold [1, 3–6]. Moreover, pronounced Wigner-cusp-like structures have been found in the energy dependence of the DA cross section [2, 7]. The explanation of these phenomena has been a challenge for the theory for some time. A variety of theoretical methods and models has been developed

and employed, for example, the close-coupling method [8], the R -matrix method [9–13], the Fano-Feshbach resonance approach [14–19], or effective-range-type models [20]. The so-called nonlocal resonance model [12, 14] (the name originates from the fact that the effective potential for the nuclear motion in the resonance state is nonlocal) derived from the Fano-Feshbach approach has been particularly successful in providing a unified description of VE and DA processes in the collision of low-energy electrons with HX ($X = \text{F, Cl, Br, I}$) [15–19]. Recently the associative detachment cross section in $\text{H} + \text{Cl}^-$ collisions has been calculated within the nonlocal resonance model as well [22].

The nonlocal resonance model is formulated in terms of a discrete (localized) electronic state and an electronic scattering continuum. These electronic basis states are assumed to be diabatic, i.e., slowly varying functions of the internuclear distance R . Basic quantities in the nonlocal resonance model are the energy-dependent decay width of the resonance

$$\Gamma(E, R) = 2\pi |V_{dE}(R)|^2 \quad (1)$$

and the associated level-shift function

$$\Delta(E, R) = \frac{1}{2\pi} \text{P} \int dE' \frac{\Gamma(E', R)}{E - E'} \quad (2)$$

Here P denotes the principal value of the integral and $V_{dE}(R)$ is the discrete-continuum coupling matrix element.

In the nonlocal resonance model the energy dependence of Γ is given by Wigner's threshold law, that is

$$\Gamma(E) \sim E^\alpha \quad (3)$$

at low energies. The energy dependence of Γ and the resulting nonanalyticity of $\Delta(E)$ are explicitly taken into account. Therefore the interplay of resonance and threshold effects is included in this formulation. This feature has been found to be essential for the description of the threshold phenomena in electron collisions with hydrogen halides (see [21] for a review).

In the absence of long-range electron-molecule scattering potentials, the threshold exponent α in Eq. (3) is given by

* Dedicated to Prof. Dr. Wilfried Meyer on the occasion of his 60th birthday

Correspondence to: W. Domcke
e-mail: Domcke@theochem.uni-duesseldorf.de

$$\alpha = l + \frac{1}{2} \quad (4)$$

where l denotes the lowest partial wave into which the resonance can decay according to symmetry selection rules ($l = 0$ for the $2^2\Sigma^+$ shape resonances of the hydrogen halides). As is well known, the long-range dipole potential modifies the threshold exponent, leading to non-half-integral values of α [14, 23]. The value of α for the hydrogen halides is thus determined by the dipole moments of these molecules.

Since the dipole moments of the hydrogen halides depend on the internuclear distance, the threshold exponent also is a function of the internuclear distance: $\alpha = \alpha(R)$. In all calculations performed so far, the threshold exponent has been approximated by its value at the equilibrium distance of the target molecule, i.e., $\alpha = \alpha(R_0)$. This approximation simplifies the calculations. On the other hand, the variation of the dipole moment with R is significant for the lighter hydrogen halides, which become very polar for intermediate internuclear distances [24, 25]. One would expect that the consideration of the variation of α with R should lead to an improved description of the threshold effects, in particular for HF and HCl.

In the present work we have determined the threshold exponent as a function of R for HCl, HBr, and HI. The computational scheme for the treatment of the nuclear dynamics in the nonlocal energy-dependent potential of the resonance state has been extended to allow for a variable threshold exponent $\alpha(R)$. It is shown that the variation of α with R has significant effects for low-energy electron-HCl scattering. The generalized model provides an improved description of the vibrational excitation functions of HCl. The effects for the less polar molecules HBr and HI are found to be minor. The electron-HF collision complex is not considered here, since the dipole moment of the HF molecule is supercritical for a certain range of internuclear distances, which requires a special treatment (see [19] for a recent application of the nonlocal theory to the electron-HF system).

2 Theory and computational methods

In the existing applications of the nonlocal resonance model to electron-HX collisions, the discrete-continuum coupling matrix element has been taken to be of the form

$$V_{dE}(R) = f(E)g(R) \quad (5)$$

The dependence of V_{dE} on energy is thus assumed to be the same for all internuclear distances, which is, of course, a rather restrictive assumption.

In the model of Domcke and Mündel [15], henceforth referred to as DM, the function $f(E)$ has been represented by the analytic expression

$$f(E) = (2\pi)^{-\frac{1}{2}} A^{\frac{1}{2}} (E/B)^{\alpha} e^{-E/B} \quad (6)$$

Here α is the threshold exponent evaluated with the dipole moment at the equilibrium distance R_0 of the target molecule. The parameter A determines the overall strength of the discrete-continuum coupling, and B is a high-energy cut-off parameter. For the function $g(R)$, various forms have been chosen [15, 17, 26]. The unknown parameters have been determined by fitting the scattering phaseshift in the fixed-nuclei approximation to ab initio calculations [15, 17].

In the present work we replace the DM ansatz (5, 6) by the more general form

$$V_{dE}(R) = f(E, R)g(R) \quad (7)$$

$$f(E; R) = (2\pi)^{-\frac{1}{2}} A^{\frac{1}{2}} (E/B)^{\alpha(R)} e^{-E\beta(R)/B} \quad (8)$$

where $\alpha(R)$ and $\beta(R)$ can be arbitrary functions. The dependence of V_{dE} on energy is now an explicit function of the internuclear distance. The R -dependent threshold exponent $\alpha(R)$ is determined by the dipole moment function of the target molecule, which is well known for the hydrogen halides [24, 25]. The function $\beta(R)$ accounts for a dependence of the high-energy cut-off parameter on the internuclear distance. Since the aim of this paper is to reveal the effect of the R -dependence of α , we have put $\beta(R) = 1$ in the calculations.

The energy-dependent and nonlocal part of the effective potential for the nuclear motion in the resonant state is given by the following expression [21]:

$$F(E, R, R') = \Delta(E, R, R') - \frac{i}{2} \Gamma(E, R, R') \quad (9)$$

where

$$\Delta(E, R, R') = \sum_n \chi_n(R)g(R)\delta(E - E_n, R, R')\chi_n(R')g(R') \quad (10)$$

and

$$\Gamma(E, R, R') = \sum_n \chi_n(R)g(R)\gamma(E - E_n, R, R')\chi_n(R')g(R') \quad (11)$$

Here

$$\delta(E, R, R') = \frac{A}{2\pi} \mathbf{P} \int_0^{\infty} dE' \frac{(E'/B)^{(\alpha(R)+\alpha(R'))/2} e^{-E'(\beta(R)+\beta(R'))/2B}}{E - E'} \quad (12)$$

and

$$\gamma(E, R, R') = A(E/B)^{(\alpha(R)+\alpha(R'))/2} e^{-E(\beta(R)+\beta(R'))/2B} \quad (13)$$

where the $\chi_n(R)$ are eigenstates of the target molecule and the E_n their energies.

With the DM ansatz (5), the integral kernels $\delta(E, R, R')$ and $\gamma(E, R, R')$ are independent of R and R' , which simplifies the calculations considerably. The main complication introduced by the more general ansatz (7) is the fact that the kernel $\delta(E, R, R')$ is not separable in R and R' ; see Eq. (12). We may expect, however, that for reasonably smooth functions $\alpha(R)$ and $\beta(R)$ a sufficiently accurate separable approximation exists. This approximation is the key for an efficient computational algorithm for the solution of the scattering problem with the nonlocal potential operator (9).

Here we show that the kernel $\delta(E, R, R')$ can be approximated by the expression

$$\delta(E, R, R') \sim \sum_{k=1}^N B_k(E, R)B_k(E, R') \quad (14)$$

with a very small number N of terms. For the construction of this separable approximation we use the so-called Bateman expansion [27], widely used in nuclear physics.

The idea of the Bateman expansion is as follows: for the kernel $V(X, Y)$ of any nonlocal operator, a new kernel $V_1(X, Y)$ is defined as

$$V_1(X, Y) = V(X, Y) - \frac{V(X, Y_1)V(X_1, Y)}{V(X_1, Y_1)} \quad (15)$$

where X_1 and Y_1 are properly chosen points in the range of the potential V . Since for any X and Y

$$V_1(X, Y_1) = 0 \quad (16)$$

and

$$V_1(X_1, Y) = 0 \quad (17)$$

the first Bateman approximation, $B_1(X, Y)$

$$V(X, Y) \sim B_1(X, Y) = \frac{V(X, Y_1)V(X_1, Y)}{V(X_1, Y_1)} \quad (18)$$

coincides with the exact nonseparable potential at two lines: $X = X_1$ and $Y = Y_1$. The second Bateman approximation is defined similarly as a sum of two terms

$$V(X, Y) \sim B_1(X, Y) + B_2(X, Y) \quad (19)$$

where

$$B_2(X, Y) = \frac{V_1(X, Y_2)V_1(X_2, Y)}{V_1(X_2, Y_2)} \quad (20)$$

which coincides with the original potential at the lines: $X = X_1$, $X = X_2$, $Y = Y_1$, and $Y = Y_2$. This procedure is repeated until the required accuracy is obtained. It should be stressed that the resultant approximation is a sum of terms which are separable in the variables R and R' . The energy dependence, which is crucial for the proper description of threshold effects, is treated exactly.

The Bateman technique requires the specification of the points X_1, X_2 , etc. As a natural choice of the points X_1, Y_1 one may set $X_1 = Y_1 = R_0$, where R_0 is the equilibrium distance of the target molecule. It appears that the first Bateman approximation, $N = 1$, yields results correct to four significant figures not only for HI, for which the threshold exponent changes in the limits 0.468–0.5 for the R of interest, but also for HBr, which has a stronger dipole moment and for which the threshold exponent changes over a broader range of values: 0.386–0.5. For HCl, with the strongest dipole moment, two terms were needed to approximate the potential to three significant digits. The choice of the second Bateman point in the case of HCl was not crucial; the quality of the approximation was found to be nearly independent of the choice of X_2, Y_2 .

The Bateman expansion has been implemented into the code for the solution of the nuclear scattering problem with the Schwinger-Lanczos method [17, 28]. The amount of numerical work needed for calculations with R -dependent threshold exponent $\alpha(R)$ is somewhat higher than that required for constant α . Nevertheless, the calculations are still very fast and the cross sections can be determined to any desired accuracy.

3 Results and discussion

For the three molecules considered here, HCl, HBr, and HI, an analytic formula for the dipole moment function $D(R)$ has been given by Ogilvie et al. [25]. For a given dipole moment D , the threshold exponent α can straightforwardly be calculated via the diagonalization of a tridiagonal matrix [29]. The resulting functions $\alpha(R)$ for HCl, HBr, and HI are displayed in Fig. 1. While the deviations of α from the s -wave value $1/2$ are minor for HI and moderate for HBr, we observe a strong variation of α with R for HCl.

We have performed calculations for VE and DA cross sections, using previously developed nonlocal resonance models [15, 17, 18]. In all three cases the constant threshold exponent $[\alpha(R_0) = 0.36, 0.42, 0.48$ for HCl, HBr, HI, respectively] has been replaced by the $\alpha(R)$ functions of Fig. 1.

The DA cross section obtained for HCl in the $v = 0$ state is shown in Fig. 2 in comparison with the DM result. One can see that the effect of the variation of α with R is marginal for the DA cross section. This result is in agreement with previous findings which indicated that the shape and magnitude of the DA cross section is rather insensitive to details of the model [30, 31].

Figure 3 gives an overview of the $0 \rightarrow 1$, $0 \rightarrow 2$, and $0 \rightarrow 3$ integral VE cross sections for HCl. The present variable- α results (full curves) are compared with the DM

results (dashed curves). While the broad shape-resonance feature near 2.5 eV collision energy is not much affected by the variation of α with R , the shape and intensity of the threshold peaks change significantly. For the $0 \rightarrow 1$ channel, in particular, the cross section at threshold is strongly enhanced (by more than a factor of two).

Figure 4 displays the threshold peak in the $0 \rightarrow 1$ channel on an enlarged energy scale, in comparison with (nonnormalized) experimental data of Schafer and Allan [5]. It is seen that the shape of the calculated threshold peak is in much better agreement with the experimental data than the original DM result. As emphasized by the authors [5], cross section measurements close to threshold are extremely difficult and uncertainties up to a factor of two are to be expected. The calculation predicts a peak value of about 20 \AA^2 for the integral $0 \rightarrow 1$ cross section.

For the $0 \rightarrow 2$ channel we find a pronounced double-peak structure in the threshold region (Fig. 3b). Indications of a multiple-peak structure have indeed been seen in the measurements of Cvejanović [6]. The splitting of the threshold peak in the $0 \rightarrow 2$ channel is closely related to oscillatory fine structure in the $0 \rightarrow 1$ cross section converging towards the DA threshold [5, 6]. This fine structure is not quantitatively reproduced by the DM as well as by the present model owing to deficiencies

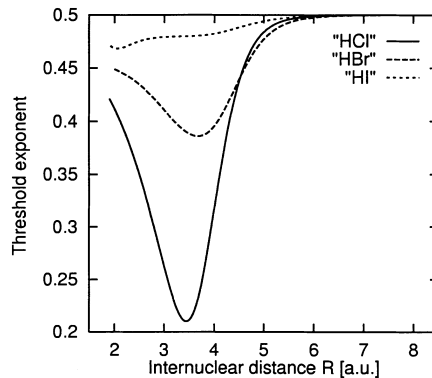


Fig. 1. Threshold exponent as a function of the internuclear distance for $e + \text{HCl}$ (full curve), $e + \text{HBr}$ (long dashes), and $e + \text{HI}$ (short dashes)

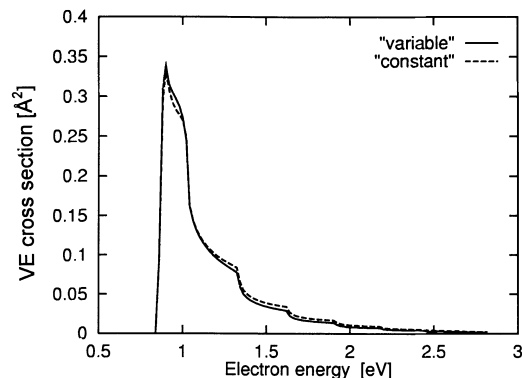


Fig. 2. Dissociative attachment cross section in HCl ($v = 0$). The cross section obtained with variable α (full curve) is compared with the cross section obtained with constant α (dashed curve)

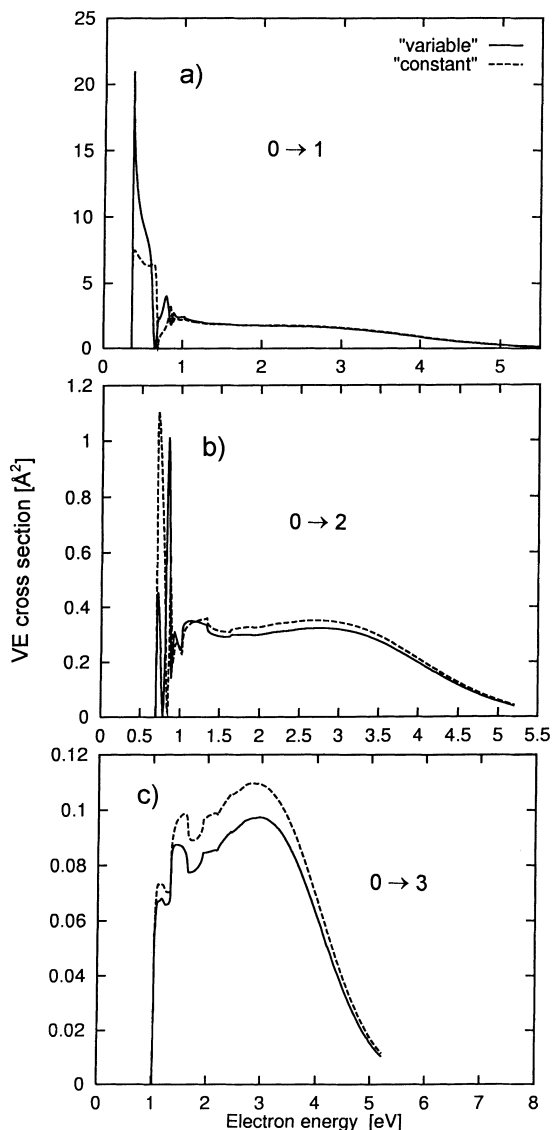


Fig. 3. Integral vibrational excitation (VE) cross section in HCl for the **a** $0 \rightarrow 1$, **b** $0 \rightarrow 2$, and **c** $0 \rightarrow 3$ channels, obtained with the variable- α (*full curve*) and fixed- α (*dashed curve*) calculations

of the HCl^- potential energy function at large internuclear distances. Improvement of the model to obtain a better description of the long-range part of the HCl^- potential function will be the subject of future work.

In Fig. 5 the integral $0 \rightarrow 3$ VE cross section obtained in the present calculation is compared with experimental data of Schafer and Allan (the latter represent the sum of forward and backward cross sections). In this channel (as well as in all higher channels) threshold peaks are absent. The cross sections are dominated by the broad shape resonance near 2.5 eV collision energy. It is seen that the threshold cusp structures in the $0 \rightarrow 3$ cross section are qualitatively reproduced by the calculation.

In the calculations for $e + \text{HBr}$ and $e + \text{HI}$ the replacement of α by $\alpha(R)$ leads to only minor changes of the cross sections for all channels. Therefore these results are not shown here. It can be concluded that these col-

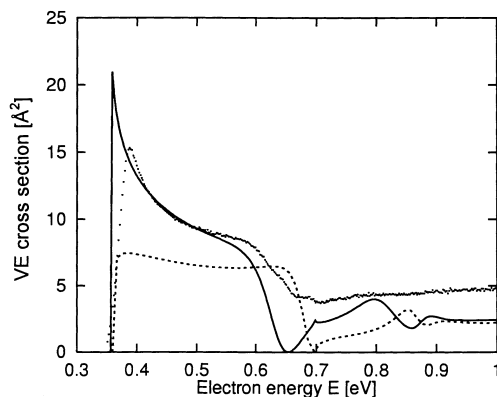


Fig. 4. Expanded view of the threshold peak in the $0 \rightarrow 1$ VE cross section of HCl, obtained with the variable- α calculation (*full curve*). The *dots* represent the $0 \rightarrow 1$ excitation function measured by Schafer and Allan [5]. The normalization of the experimental data is arbitrary. The *dashed line* represents the Domcke-Mündel (DM) result [15]

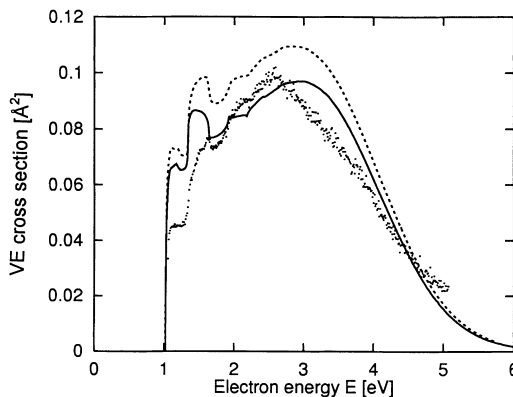


Fig. 5. The $0 \rightarrow 3$ VE cross section in HCl, obtained with the variable- α model, in comparison with the (non-normalized) experimental data of Schafer and Allan [5]. The *dashed line* represents the DM result [15]

lision systems are accurately described by the nonlocal resonance model with constant threshold exponent.

In summary, we have shown that the variation of the threshold exponent with the internuclear distance is a relevant feature for the $e + \text{HCl}$ system. Inclusion of the R -dependence of α leads to a substantial improvement in the description of the threshold peak in the $0 \rightarrow 1$ VE cross section. It appears that the mechanisms behind the much discussed threshold peaks in the electron-HX cross sections are now well understood, not only qualitatively, but also in the sense of quantitative predictions of cross sections.

References

1. Rohr K, Linder F (1976) *J Phys B* 9:2521
2. Abouaf R, Teillet-Billy D (1977) *J Phys B* 10:2261
3. Rohr K (1978) *J Phys B* 11:1849
4. Knoth G, Rädle M, Gote M, Ehrhardt H, Jung K (1989) *J Phys B* 22:299, 1455
5. Schafer O, Allan M (1991) *J Phys B* 24:3069

6. Cvejanović S (1993) In: 18th Int Conf on Electronic and Atomic Collisions (ICPEAC), Aarhus (book of invited papers)
7. Abouaf R, Teillet-Billy D (1980) Chem Phys Lett 73:106
8. Snitchler G, Norcross D, Jain A, Alston S (1990) Phys Rev A 42:671
9. Morgan LA, Burke PG (1988) J Phys B 21:2091
10. Morgan LA, Burke PG, Gillan CJ (1990) J Phys B 23:99
11. Fandreyer R, Burke PG, Morgan LA, Gillan CJ (1993) J Phys B 26:3625
12. Fabrikant II (1990) Comments At Mol Phys 24:37
13. Thümmel HT, Nesbet RK, Peyerimhoff SD (1993) J Phys B 26:1233
14. Domcke W, Cederbaum LS (1981) J Phys B 14:149
15. Domcke W, Mündel C (1985) J Phys B 18:4491
16. (a) Kalin SA, Kazansky AK (1990) J Phys B 23:4377; (b) Fabrikant II, Kalin SA, Kazansky AK (1991) J Chem Phys 95:4966
17. Horáček J, Domcke W (1996) Phys Rev A 53:2262
18. Horáček J, Domcke W, Nakamura H (1997) Z Phys D 42:181
19. Gallup GA, Xu Y, Fabrikant II (1998) Phys Rev A 57: 2596
20. Teillet-Billy D, Gauyacq JP (1984) J Phys B 17:4041
21. Domcke W (1991) Phys Rep 208:97
22. Čížek M, Horáček J, Domcke W (unpublished)
23. O'Malley TF (1965) Phys Rev A 137:1668
24. Werner H-J, Rosmus P (1980) J Chem Phys 73:2319
25. Ogilvie JF, Rodwell WR, Tipping RH (1980) J Chem Phys 73:5221
26. Gertitschke PL, Domcke W (1994) Z Phys D 31:171
27. Bateman H (1922) Proc R Soc Lond Ser A 100:441
28. Horáček J, Gemperle F, Meyer H-D (1996) J Chem Phys 104:8433
29. Crawford OH (1967) Proc Phys Soc 91:279
30. Fabrikant II (1986) Z Phys D 3:401
31. Domcke W (1990) In: Herzenberg A (ed) Aspects of electron-molecule scattering and photoionization. American Institute of Physics, New York, p 169